Theoretical study of the HNS+/HSN+ radical cations

ARTICLE *in* JOURNAL OF MOLECULAR STRUCTURE THEOCHEM · JANUARY 2002

Impact Factor: 1.37 · DOI: 10.1016/S0166-1280(01)00676-5

8 AUTHORS, INCLUDING:

Nejm-Eddine Jaidane
University of Tunis El Manar
110 PUBLICATIONS **550** CITATIONS
SEE PROFILE

Chambaud Gilberte
Université Paris-Est Marne-la-Vallée
182 PUBLICATIONS **1,429** CITATIONS
SEE PROFILE

ELSEVIER

Journal of Molecular Structure (Theochem) 577 (2002) 255–265

THEO CHEM

www.elsevier.com/locate/theochem

Theoretical study of the HNS^+/HSN^+ radical cations

S. Ben Yaghlane[a], S. Lahmar[a], N. Jaidane[a], Z. Ben Lakhdar[a], G. Chambaud[b,*], P. Rosmus[b], J.M. Robbe[c], A. Spielfiedel[d]

[a]*Laboratoire de Physique Atomique et Moléculaire, Faculté des Sciences de Tunis, Tunisie*
[b]*Laboratoire de Chimie Théorique, Université de Marne la Vallée, Cité Descartes, B, Bd Descartes, Champs sur Marne, 77454 Marne la Vallée, France*
[c]*Laboratoire de Physique des Lasers, Atomes et Molécules, Université de Lille.1, Lille, France*
[d]*Damap, Observatoire de Paris-Meudon, Paris, France*

Received 9 July 2001; accepted 30 July 2001

Abstract

The three dimensional CASSCF-MRCI potential energy functions have been calculated for the X^2A' and A^2A'' electronic states of HNS^+ and for the X^2A' state of the HSN^+ isomer. In HNS^+, the two lowest states form a linear-bent Renner–Teller pair, the MRCI barrier to linearity for the X-state has been calculated to be 1876 cm^{-1}. Both isomers possess a conical intersection resulting from the crossing between the $^2\Sigma^+$ and $^2\Pi$ states along the colinear $H(^2S) + NS^+(X^1\Sigma^+)$ dissociation path. The minima of both isomers are found to be separated by a large barrier of 18,042 cm^{-1} (CASSCF), the HNS^+ isomer is calculated to be more stable than HSN^+ by 12,202 cm^{-1} (34.9 kcal/mol) (RCCSD(T)). The proton affinity of the NS radical ($NS(X^2\Pi) + H^+$) has been calculated to be 7.59 eV (RCCSD(T)), the dissociation energy of $HNS^+ \rightarrow H(^2S) + NS^+(X^1\Sigma^+)$ to be 2.86 eV (RCCSD(T)). Due to several low-lying electronic states of NS^+, the protonation and the exothermic charge transfer reactions $H^+ + NS \rightarrow H + NS^+$ are found to proceed via very complex reaction paths including vibronic and spin–orbit couplings. The results of Renner–Teller variational calculations of the rovibronic levels for the electronic ground state of HNS^+ are presented. The onset of this coupling is calculated already in the first bending overtone of the X-state. Also the vibrational levels obtained variationally for the X^2A' state of the HSN^+ isomer are given.

Keywords: Potential energy functions; Renner–Teller spectroscopy; Isomerisation; Protonation

1. Introduction

The protonated diatomics such as HCO^+, HCS^+ or HN_2^+ are present in many molecular clouds in star forming regions [1]. Recently, observational evidence has been reported in a sample of 10 clouds that a comparison of the spectra of such ions and neutral species present in the same cloud could serve to detect the existence of a magnetic field [1]. The measurements of the distribution of the HCO^+ ion in the nebula OH231.8 + 4.2, known for its active chemistry, suggest that the ion is formed by shock-induced reactions there [2]. Ion-neutral reactions initiate the formation of molecules involving oxygen and carbon, and their abundances are better explained by existing models than those of the sulphur bearing molecules [3]. The NS radical is one of the fundamental species related to interstellar nitrogen [4] and sulphur chemistry [5]. It was first identified in Sgr B2 [6], and

* Corresponding author. Tel.: +33-160-95-73-03; fax: +33-160-95-73-20.
E-mail address: g.chambaud@univ-mlv.fr (G. Chambaud).

0166-1280/02/$ - see front matter
PII: S0166-1280(01)00676-5

Table 1
Geometries and CASSCF energies for the minima and the saddle points on X^2A' and A^2A'' potential energy functions of the HNS^+/HSN^+ system (cf. Fig. 1)

	R_{NS}[a]	R_{NH}[a]	α_{HNS}[b]	Energy[c]
$HNS^+(X^2A')$	2.83	1.96	129.50	−452.343798
$HNS^+(A^2A'')$	2.78	1.93	180.00	−452.332924
Isomerisation barrier	2.98	2.74	61.50	−452.261589
Activation barrier	2.79	3.5	116.5	−452.272045
Dissociation limit	2.74	12	180.00	−452.282025
$HSN^+(X^2A')$	2.93	2.63	100.16	−452.297057

[a] In bohr.
[b] In °.
[c] In a.u.

studied mainly in the regions of massive star formation [3]. The NS has been found in 12 giant molecular clouds [3], detected in cold dark stars [7], in circumstellar envelopes [2] and in Hale–Bopp comet [8]. A possible precursor in the latter case could be HNS [8], which is expected to be stable at low temperatures of cometary nuclei, but has not yet been studied in laboratory with a spectroscopic precision needed for astrophysical purposes. If HNS is present in comets then it will be ionised in comet tails. Under the dark cloud conditions, McGonagle et al. [7] suggested a model for the formation mechanism of NS involving HNS^+: $HNS^+ + e \rightarrow NS + H$ and assumed that HNS^+ can be formed (e.g.) from $NH_2^+ + S$. The NH_2^+ is thought to result from the reaction of molecular nitrogen with H_3^+. The purpose of the present contribution is to provide theoretical spectroscopic data, which could aid the experimental laboratory study of both isomers, and eventually lead to detection of the ion in the outer space.

The HNS/HSN neutral isomers have been the subject of several studies [9–16] but only little has been known about the HNS^+/HSN^+ ions, so far. Experimentally, a mass spectroscopic detection has been reported using 1,3,4-oxathiazol-2-one [17] as a precursor. The first ab initio study on this ion was performed by Bruna and Hirsch who determined at the MRD-CI level of theory [18] the equilibrium geometries of the HNS^+ and HSN^+ isomers in their X^2A' ground states. Both species were found to have bent equilibrium structures and HNS^+ was calculated to be more stable than HSN^+ by 36.4 kcal/mol. Gersdorf [19] reported results of MRCI computations of near equilibrium three dimensional potential energy and dipole moment functions in the electronic ground state and the absolute rotational line intensities. The electronically excited states have not yet been studied. The first A^2A'' excited state and the X^2A' electronic ground state of the HNS^+ isomer correlate at linearity with the $^2\Pi$ state forming a Renner–Teller pair. Hence calculations of rovibronic levels are required to go beyond the Born–Oppenheimer approximation and to take into account the angular momenta coupling effects. For linear configuration of the HSN^+ isomer, the saddle point region of the $^2\Pi$ state is perturbed by a $^2\Sigma^+$state, i.e. three states are coupled. For this isomer only, the vibrational problem of the X-state has been treated variationally. The proton affinity of NS has not yet been known. Since the ionisation energy of NS amounts to 8.87 eV [20], i.e. it is much lower than that of the H atom, this reaction proceeds in a very complex way due to interactions between states correlating with several asymptotes lying below the $H^+ + NS(X^2\Pi)$ dissociation limit.

In Section 2, we describe the calculations used to map the energy positions of the minima and saddle points on the potential energy surfaces of the $(HNS)^+$ system in its lowest electronic states. In Section 3, the results for the diatomic fragments NS and NS^+ are presented allowing to assess the accuracy of the data obtained for the triatomic ion. In Section 4 spectroscopic data for HNS^+ and its isomer are given. Finally, the protonation of NS and the charge transfer processes in the HNS^+ system are discussed in Section 5.

2. Minima and saddle points of low lying states of HNS^+/HSN^+

In the electronic calculations, we used two AO basis sets. The basis set A consisted of the s,p,d,f subset of the correlation consistent polarized valence quadruple-zeta (cc-pVQZ) set of Dunning [21]. The basis set B (full cc-pV5Z) [21] was used only for some selected computations as described in the following paragraphs.

In order to understand the shape of the potential energy surfaces of the $(HNS)^+$ system in the lowest electronic states, we first performed preliminary calculations using complete active space self-consistent field (CASSCF) approach [22,23] with the code MOLPRO.[1]

[1] All calculations have been performed with the MOLPRO programs written by H.J. Werner, P.J. Knowles, with contributions of J. Amlöf, R.D. Amos, S.T. Elbert, et al.

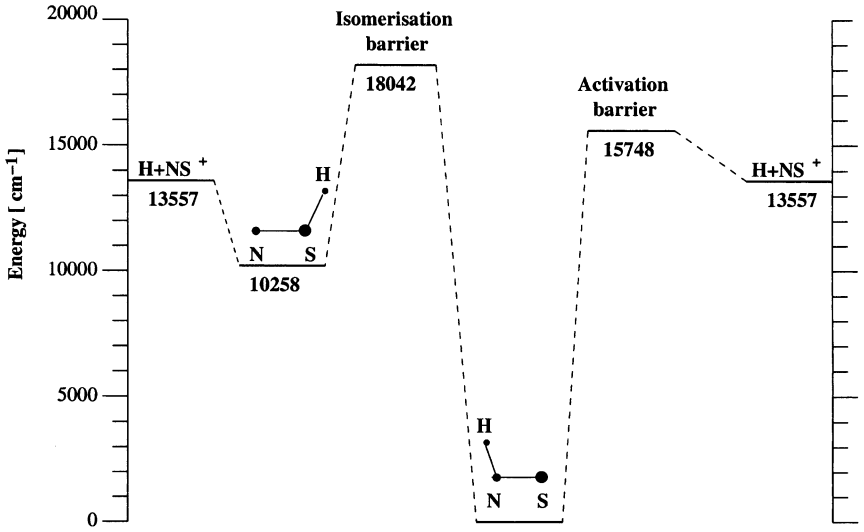

Fig. 1. Schematic CASSCF potential energy profile for the HNS^+/HSN^+ system of the X^2A' ground state.

The computations were done for 318 geometries in a coordinate system where the molecule lies in the *xy* plane, with the nitrogen atom located in the origin, the sulphur atom moving on the *x* axis and the H in the geometry range: $-8.0\ \text{bohr} \leq x_H \leq 10.0\ \text{bohr}$ and $1.0\ \text{bohr} \leq y_H \leq 3.2\ \text{bohr}$. The minima and saddle points are given in Table 1 and a scheme related to their energy positions for the lowest $^2A'$ state is shown

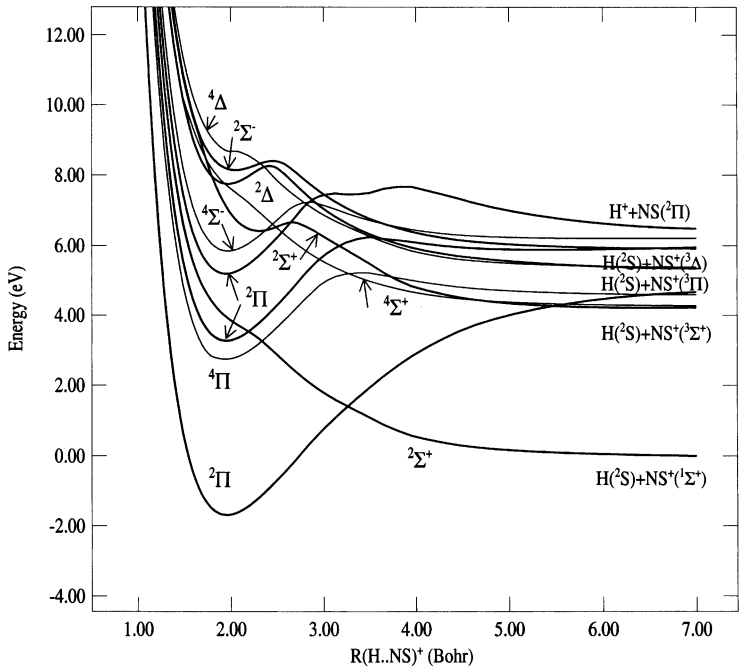

Fig. 2. Linear dissociation of HNS^+ along the R_{NH} distance ($R_{NS} = 2.74$ bohr) for the low electronic states.

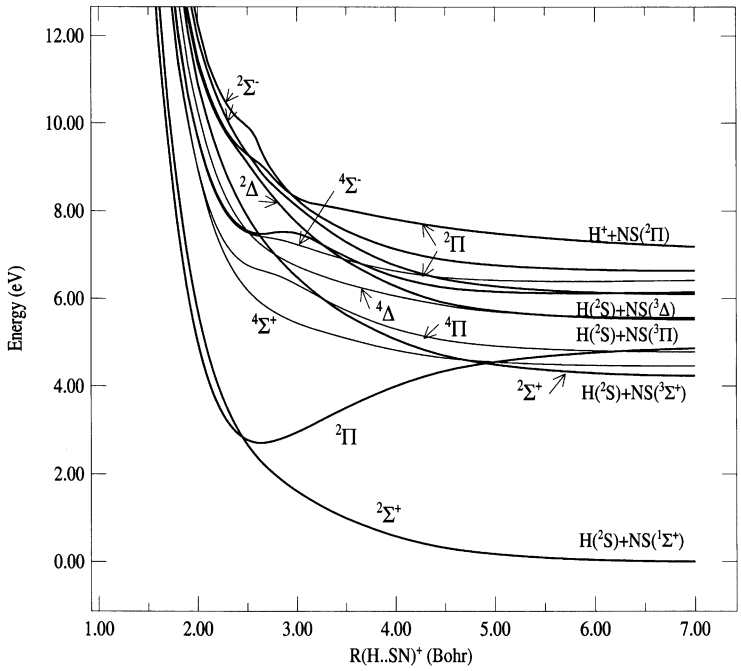

Fig. 3. Linear dissociation of HSN^+ along the R_{SH} distance ($R_{SN} = 2.74$ bohr) for the low electronic states.

in Fig. 1. In these CASSCF calculations, the core orbitals were kept doubly occupied and the nine valence orbitals formed the active space. The $^2A'$ and $^2A''$ states were averaged together with equal weights. Similarly, in subsequent CASSCF calculations used to map the excited states, all electronic states with same spin multiplicity were obtained by state averaged calculations. In the colinear approach $H\cdots NS^+$ (Fig. 2) or $H\cdots SN^+$ (Fig. 3), the cuts of the $^2\Sigma^+$ state correlating with the ground state of NS^+ for both orientations are repulsive, but the $^2\Pi$ state correlating with the $H(^2S) + NS^+(b^3\Pi)$ asymptote becomes strongly bound and crosses the $^2\Sigma^+$ PES. This crossing leads to conical intersections and in the case of the HNS^+ bent structure to a barrier in the entry channel of the $^2A'$ electronic ground state. This barrier has been calculated to be about 2200 cm^{-1}. The isomerisation barrier of about 18,000 cm^{-1} lies above the first dissociation threshold of the $^2A'$ state. In Fig. 4, the cuts along the bending coordinates show that in the HNS^+ structure the first two electronic states form a linear/bent Renner–Teller system (cf. Section 3), whereas the HSN^+ structure, not represented here, possesses close to the linear saddle point a conical intersection. The X^2A' state of this HSN^+ structure is strongly bent and energetically well separated from that region. Nevertheless, it correlates diabatically to the same asymptote as the X^2A' state of HNS^+.

3. Spectroscopic data of NS and NS^+

The potential energy surfaces for the Renner–Teller pair of HNS^+ and the X^2A' state of HSN^+ have been generated by an internally contracted MRCI [24,25] approach using all configurations of the valence CASSCF wavefunction as a reference and the basis set A. Since no experimental data are available for the triatomic ion, we have performed computations for NS and NS^+ with the above approach in order to check its accuracy. Additional computations were done with the basis set B and the partially restricted coupled cluster variant RCCSD(T) [26] which includes single and double excitation operators and approximates the effect of connected triple substitutions by means of perturbation theory. For the NS ground state, very accurate experimental spectroscopic data exist [27] and allow a comparison with the present results. Since the core-valence

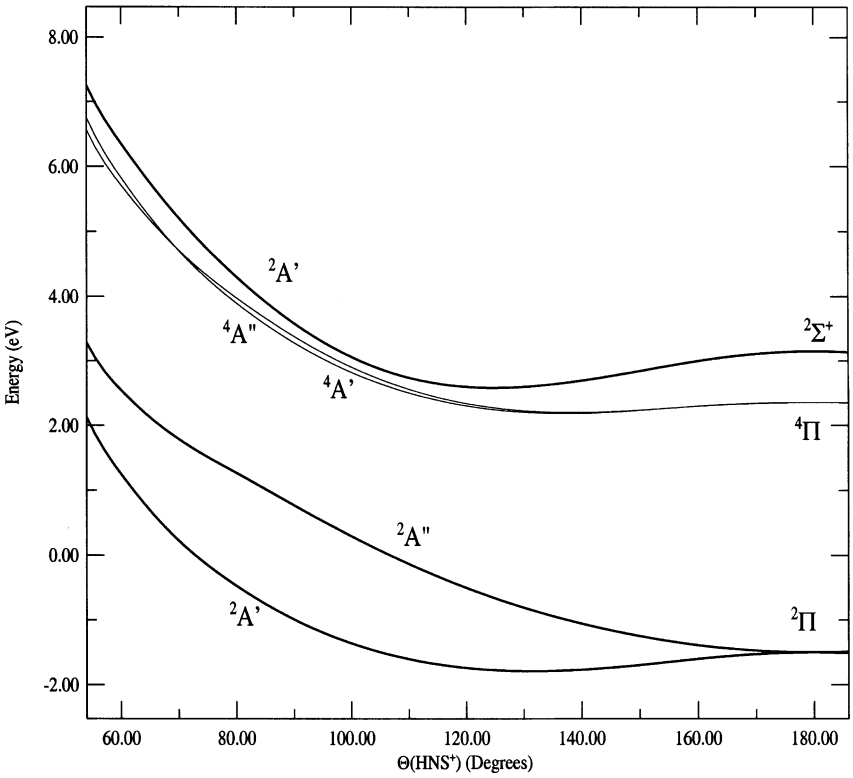

Fig. 4. Cut of the potential energy functions of the low electronic states of HNS^+ along the bending coordinate ($R_{NH} = 1.95$ bohr and $R_{NS} = 2.8$ bohr).

correlation energy contributions have been neglected, the RCCSD(T) distance is larger by 0.002 Å than the experimental value, the harmonic wavenumber by 22 cm^{-1}, indicating that the *r*-dependent correlation energy has not been fully accounted for even in these large scale computations. The MRCI distance is too large and the ω_e too small. The Davidson correction is not improving the agreement with experiment. The electronic ground state of NS^+ has been studied only by low resolution photoelectron spectroscopy [20] and no accurate data are available for comparison. The experimental ionisation energy $IE_o$of NS has been determined to be 8.87 eV [20], the MRCI value has been calculated to be 8.40 eV, the RCCSD(T) value to be 8.78 eV. The difference between the ionisation energies of NS and H atom amounts to 4.735 eV. According to Table 2, three triplet states lie below this value, i.e. below the $H^+ + NS$ asymptote. As will be discussed in Section 6, the fact that there are nine electronic states of NS^+ below 6 eV (cf. Table 2) with the corresponding asymptotes, leads to many molecular states of the triatomic ion, which interfere with the PEF correlating with the $H^+ + NS$ dissociation limit. Since none of the excited states has been experimentally known, the data in Table 2 give helpful information for spectroscopic studies of this diatomic ion. In early MRD-CI computations of the excited states, Karna and Grein [28] has used a double-zeta plus polarization plus diffuse basis set. The present more accurate data deviate in the excitation energies by up to 0.5 eV, the ω_e by up to about 70 cm^{-1}. The CEPA r_e for the ground state of NS^+ [29] of 1.439 Å is in good agreement with the present RCCSD(T) result.

4. Potential energy functions and spectroscopic constants of HNS^+ and HSN^+

The Renner–Teller PEF's of HNS^+ have been

Table 2
Spectroscopic constants for the ground state of NS and the low lying electronic states of NS^+

	State	Method	Basis	r_e(Å)	B_e(cm^{-1})	ω_e (cm^{-1})	$\omega_e x_e$ (cm^{-1})	T_e (eV)
NS	$X^2\Pi$	MRCI	A	1.507	0.757	1192.2	7.60	
		MRCI + Q[b]	A	1.508	0.756	1183.1	7.55	
		RCCSD(T)	B	1.496	0.774	1240.7	7.6	
		Exp[a]		1.494	0.775	1218.7	7.2	
NS^+	$X^1\Sigma^+$	MRCI	A	1.446	0.822	1389.4	8.0	0
		MRCI + Q	A	1.448	0.819	1398.1	8.1	
		RCCSD(T)	B	1.441	0.834	1426.9	7.8	
		Exp[a]		1.440		1415.0		
	$1^3\Sigma^+$	MRCI	A	1.638	0.641	880.1	7.8	3.45
		MRCI + Q	A	1.640	0.639	876.0	7.8	3.37
	$1^3\Pi$	MRCI	A	1.503	0.760	1144.6	9.9	4.52
		MRCI + Q	A	1.504	0.760	1147.0	9.5	4.40
	$1^3\Delta$	MRCI	A	1.623	0.652	935.4	6.8	4.55
		MRCI + Q	A	1.624	0.651	933.8	9.9	4.42
	$1^3\Sigma^-$	MRCI	A	1.619	0.656	946.6	6.6	5.27
		MRCI + Q	A	1.619	0.656	948.4	6.6	5.16
	$1^5\Sigma^+$	MRCI	A	1.977	0.440	470.1	6.0	5.34
		MRCI + Q	A	1.975	0.440	476.7	5.9	5.25
	$1^1\Sigma^-$	MRCI	A	1.617	0.658	949.9	6.5	5.48
		MRCI + Q	A	1.616	0.658	957.0	6.5	5.28
	$1^1\Pi$	MRCI	A	1.499	0.765	1156.5	8.8	5.73
		MRCI + Q	A	1.501	0.763	1149.5	8.9	5.61
	$1^1\Delta$	MRCI	A	1.608	0.665	1394.3	7.0	5.92
		MRCI + Q	A	1.606	0.667	1390.0	7.1	5.73

[b] Including Davidson correction; total energies at r_e of the $X^2\Pi$ state of NS are −452.324449 a.u. (MRCI), −452.352845 a.u. (MRCI + Q), −452.372334 a.u. (RCCSD(T)); total energies at r_e of the $X^1\Sigma$ state of NS are −452.015666 a.u. (MRCI), −452.033625 a.u. (MRCI + Q), −452.049438 a.u. (RCCSD(T)).

[a] Ref. [27].

mapped by CASSCF-MRCI approach with the basis set A for 120 geometries. The MRCI energies were fit to a sextic polynomial expansion in the displacement coordinates:

$$V(r_{NS}, r_{NH}, \alpha_{HNS}) = \sum_{i,j,k} C_{ijk}(R_1)^i(R_2)^j\Theta^k$$

The coordinates R_i and Θ are defined as: $R_1 = r_{NS} - r_{NS}^{ref}$, $R_2 = r_{NH} - r_{NH}^{ref}$ and $\Theta = \alpha - \alpha_{HNS}^{ref}$ (in radians), with the calculated equilibrium geometry as reference. The analytic PEF's can be obtained on request.[2] These PEF's are valid in the geometry range of 2.675 bohr $\leq r_{NS} \leq$ 3.2 bohr, 1.74 bohr $\leq r_{NH} \leq$ 2.27 bohr, and $90° \leq \alpha \leq 180°$. In both X^2A' and A^2A'' states, the electronic wave function has one dominating configuration: $X^2A'(9a'^2\ 2a''^2\ 10a')$, $A^2A''(9a'^2\ 2a''^2\ 3a'')$ for bent geometries, and $^2\Pi$ $(7\sigma^2\ 2\pi^4\ 3\pi)$ for linear geometries.

The expansions have been transformed to quartic force field in internal coordinates and by *l*-tensor algebra [30] to dimensionless normal coordinates. The MRCI spectroscopic constants calculated from the latter force field by the second order perturbation theory [31] are given in Table 3 for the HNS^+ isomer only. The ω_1 and ω_3 are associated with the stretching modes N–S and N–H, respectively, and ω_2 corresponds to the bending mode. These values can prove useful, for instance, for setting up empirical Renner–Teller Hamiltonians or in the interpretation of experimental spectra. The MRCI barrier to linearity in the X-state has been calculated to be 1876.1 cm^{-1}. In the X-state, the calculated ν_3 value of 3226 cm^{-1} lies already above this barrier. The electric dipole moment μ_e (relative to the centre of mass) in the X-state has been calculated to be 1.506 Debye.

[2] Can be downloaded from www.univ-mlv.fr and the homepage of the Theoretical Chemistry Laboratory.

Table 3
Molecular parameters and spectroscopic constants of HNS^+ and DNS^+ in the X^2A' and A^2A'' states

	$HNS^+(X^2A')$	$DNS^+(X^2A')$	$HNS^+(A^2A'')$	$DNS^+(A^2A'')$
R_{eNS} (Å)	1.485		1.463	
R_{eNH} (Å)	1.027		1.015	
α_{eHNS} (°)	132.049		180.000	
A_e (cm^{-1})	33.4272	19.1578		
B_e (cm^{-1})	0.6886	0.6141	0.6765	0.5850
C_e (cm^{-1})	0.6747	0.5951		
ω_1 (cm^{-1})	1258.8	1229.1	1324.3	1276.6
ω_2 (cm^{-1})	759.1	575.3	753.8	556.5
ω_3 (cm^{-1})	3398.1	2498.9	3596.9	2667.5
ν_1 (cm^{-1})	1239.7	1212.0	1285.9	1248.8
ν_2 (cm^{-1})	715.5	550.9	716.4	551.2
ν_3 (cm^{-1})	3226.7	2414.4	3335.8	2524.2
x_{11} (cm^{-1})	−7.6	−10.7	−8.7	−9.5
x_{22} (cm^{-1})	−20.8	−12.1	−0.7	−1.2
x_{33} (cm^{-1})	−83.3	−44.5	−114.7	−62.2
x_{12} (cm^{-1})	−0.19	−0.3	−6.2	−0.8
x_{13} (cm^{-1})	−6.6	9.1	−29.7	16.2
x_{23} (cm^{-1})	−3.1	−0.01	−16.7	−10.8
α_1^A (cm^{-1})	0.668	0.303		
α_2^A (cm^{-1})	−8.557	−3.785		
α_3^A (cm^{-1})	2.325	1.065		
α_1^B (cm^{-1})	0.005	0.003	0.004	0.003
α_2^B (cm^{-1})	−0.001	−0.001	−0.0001	−0.001
α_3^B (cm^{-1})	0.002	0.002	0.003	0.003
α_1^C (cm^{-1})	0.005	0.004		
α_2^C (cm^{-1})	0.001	0.001		
α_3^C (cm^{-1})	0.003	0.003		
τ_{AAAA} (MHz)	−17 337.62	−6089.30		
τ_{BBBB} (MHz)	−0.099	−0.09	−0.08	−0.06
τ_{CCCC} (MHz)	−0.09	−0.07		
τ_{AABB} (MHz)	4.71	8.88		
τ_{BBCC} (MHz)	−0.09	−0.07		
τ_{CCAA} (MHz)	−2.54	2.47		
κ	−0.999	−0.998		
T_{ver} (cm^{-1})	0.0	0.0	7024.13	
$G(000)$ (cm^{-1})	2677.4	2137.0	3134.0	2499.6

In order to estimate the accuracy of these MRCI constants, we have performed RCCSD(T) calculations with the basis set B to obtain the quadratic force field only. The comparison of the equilibrium geometries and harmonic wavenumbers for both isomers is presented in Tables 4 and 5. The MRCI NS equilibrium distances are calculated longer, the XH distances shorter than the corresponding more accurate RCCSD(T) values. The effect of the Davidson correction on these quantities is very small. The harmonic wavenumbers for the fundamentals of the HNS^+ isomer deviate by up to 40 cm^{-1}, the MRCI S–H stretch in HSN^+ is smaller than the RCCSD(T) value by as much as 68 cm^{-1}, this difference is reduced to 53 cm^{-1} when the Davidson correction is included. The notations for the HSN^+ isomer are as follows; ω_1 for the N–S stretch, ω_2 for the bending and ω_3 for the S–H stretch. The calculations of Gersdorf [19] yielded far too long distances in both isomers by comparison to the present results. According to the experience with similar sulphur containing species, the core-valence correlation will slightly decrease the RCCSD(T) NS distance. Considering this comparison, the vibrational transition energies

Table 4
Molecular parameters and spectroscopic constants of HNS^+ in the X^2A' state

	MRCI	MRCI + Q	RCCSD(T)
R_e^{NS} (Å)	1.4855	1.4859	1.4771
R_e^{NH} (Å)	1.0279	1.0279	1.0307
α_e^{HNS} (°)	132.050	132.474	134.352
A_e (cm^{-1})	33.4272	33.9046	36.0327
B_e (cm^{-1})	0.6886	0.6877	0.6930
C_e (cm^{-1})	0.6747	0.6740	0.6799
ω_1 (cm^{-1})	1258.8	1258.1	1281.2
ω_2 (cm^{-1})	759.0	755.0	719.4
ω_3 (cm^{-1})	3398.1	3399.8	3374.6
E_e (a.u.)	−452.609877	−452.633337	−452.651179

Table 5
Molecular parameters and spectroscopic constants of HSN^+ in the X^2A' state

	MRCI	MRCI + Q	RCCSD(T)
R_e^{SN} (Å)	1.5399	1.5433	1.5353
R_e^{SH} (Å)	1.3799	1.3805	1.3842
α_e^{HSN} (°)	99.133	98.557	98.526
A_e (cm^{-1})	9.4110	9.3652	9.3145
B_e (cm^{-1})	0.7144	0.7119	0.7194
C_e (cm^{-1})	0.6640	0.6616	0.6678
ω_1 (cm^{-1})	1040.1	1031.4	1060.3
ω_2 (cm^{-1})	839.4	830.2	814.8
ω_3 (cm^{-1})	2350.6	2365.1	2418.6
E_e (a.u.)	−452.557478	−452.578929	−452.595574

in both isomers should be accurate to within about 40 cm^{-1}. The RCCSD(T) rotational constants should be accurate to within about one to two percent.

The calculated RCCSD(T) total energies of HNS^+ and NS at their equilibrium geometries (cf. Tables 2 and 4) were used to calculate the value of 7.59 eV for the proton affinity of NS. The known energy difference between the ionisation energies of the hydrogen atom and NS (4.735 eV) allows to predict the dissociation energy of $HNS^+ \rightarrow H + NS^+(X^1\Sigma^+)$ to 2.86 eV, and of HSN^+ to 1.35 eV with an accuracy of about ±0.05 eV. The HNS^+ is more stable than

Table 6
Rovibronic levels ($N = K_a$) for the X^2A' state of HNS^+ (in cm^{-1}) (the F_1 components correspond to $J = N - 1/2$ and F_2 to $J = N + 1/2$.; the spin–orbit constant A_{SO} has been set to be 273 cm^{-1})

$v_1v_2v_3$	$N = 0$, $K_a, K_c = 0, 0$	$N = 1$, $K_a, K_c = 1, 1$		$N = 2$, $K_a, K_c = 2, 1$		$N = 3$, $K_a, K_c = 3, 1$	
		F_1	F_2	F_1	F_2	F_1	F_2
(0,0,0)	00.00	32.77	39.63	135.39	146.64	300.65	316.04
(0,1,0)	724.85	761.10	778.15	893.88	916.90	1098.02	1127.50
(1,0,0)	1240.46	1272.56	1279.16	1373.13	1383.89	1535.23	1550.18
(0,2,0)	1421.77	1420.62	1478.54	1620.47	1669.85	1884.19	1938.72
(1,1,0)	1963.82	2002.96	2014.76	2128.72	2150.57	2328.10	2356.71
(0,3,0)	2127.91	1954.81	2084.51	2311.82	2397.59	2662.50	2746.61
(2,0,0)	2465.15	2496.58	2502.95	2595.18	2605.57	2754.30	2768.82
(1,2,0)	2658.93	2668.27	2669.62	2853.62	2900.06	3109.80	3161.91
(0,4,0)	2877.73	2552.85	2615.34	3006.91	3092.95	3444.85	3531.68
(2,1,0)	3866.11	3234.48	3235.26	3346.52	3365.51	3542.74	3570.44
(0,0,1)	3237.06	3237.05	3273.21	3363.16	3374.40	3515.35	3529.21
(1,3,0)	3359.54	3196.24	3338.74	3544.86	3625.58	3883.48	3963.72
(3,0,0)	3674.20	3704.99	3711.21	3801.80	3811.75	3958.03	3972.51
(0,5,0)	3706.73	3308.19	3281.95	3776.01	3792.69	4246.12	4353.50
(2,2,0)	3879.49	3900.29	3946.37	4069.29	4111.89	4320.92	4371.32
(0,1,1)	3957.79	3993.57	4006.28	4111.16	4131.01	4296.95	4325.43
(1,4,0)	4101.83	3782.46	3853.56	4234.32	4325.17	4660.75	4765.96
(3,1,0)	4392.70	4411.33	4439.36	4549.70	4569.20	4739.18	4794.07
(1,0,1)	4481.80	4511.74	4517.77	4605.49	4615.19	4758.81	4775.16
(2,3,0)	4575.01	4459.22	4572.25	4761.65	4838.21	5098.73	5164.03
(0,6,0)	4590.22	4152.42	4174.48	4648.55	4709.49	5199.96	5288.89
(0,2,1)	4647.85	4669.02	4706.75	4838.62	4877.27	5079.46	5132.34
(4,0,0)	4868.63	4898.97	4904.99	4994.14	5004.35	5149.32	5166.26

Table 7
Rovibronic levels ($N = K$) for the A^2A'' state of HNS^+ (in cm^{-1}) (the F_1 components correspond to $J = N - 1/2$ and F_2 to $J = N + 1/2$.; the spin–orbit constant A_{SO} has been set to be 273 cm^{-1})

$v_1v_2v_3$	$K = 0$	$K = 1$		$K = 2$		$K = 3$	
		F_1	F_2	F_1	F_2	F_1	F_2
(0,1,0)	3061.74						
(0,2,0)		3711.76	3701.37				
(1,1,0)	4352.32						
(0,3,0)	4452.10			4332.12	4281.16		
(1,2,0)		4991.69	4977.27				
(0,4,0)		5147.62	5198.72			4934.57	4867.10
(2,1,0)	5633.66						
(1,3,0)	5723.21			5607.04	5565.42		
(0,5,0)	5865.10			5819.74	5853.55		

HSN^+ by 34.9 kcal/mol, in good agreement with the early calculations of Bruna and Hirsch [18]

In the Renner–Teller calculations for the HNS^+ ion, a variational approach [32] has been employed taking into account the coupling of electronic, electron spin and rovibrational angular momenta. The primitive basis set consisted in symmetry adapted products of one-dimensional vibrational, rigid rotor and electron spin functions. It comprised 14 one dimensional harmonic oscillator functions for each stretching mode and 22 associated Legendre polynomials for the bending mode. The $L_{x,y}$ operators and the geometry variation of the expectation values of the L_z, L_z^2 operators have been neglected. The expectation

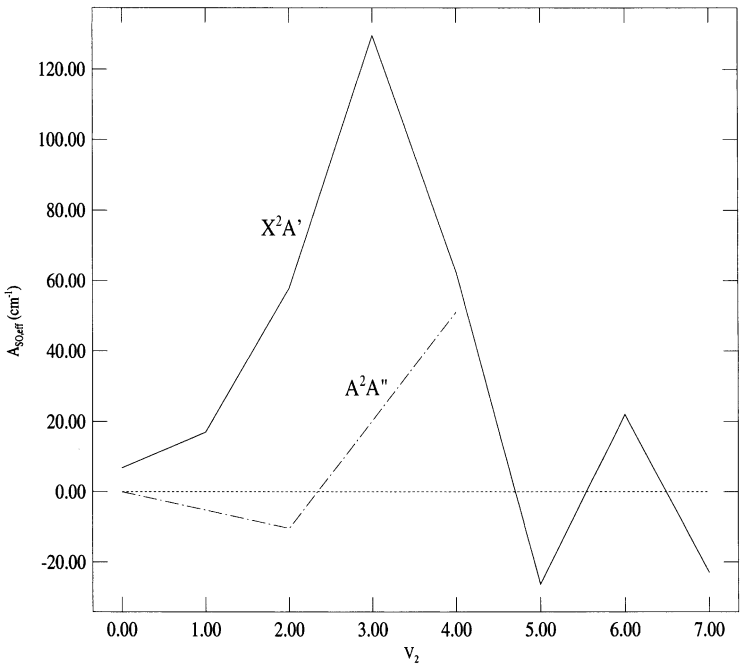

Fig. 5. Saw-tooth pattern of the spin splittings (for states with $N = 1$) in the pure bending levels $(0,v_2,0)$ of both components of the Renner–Teller HNS^+ system.

Table 8
Calculated vibrational energy levels ($N = 0$; $K_a, K_c = 0, 0$) of HSN^+ in the ground state (in cm^{-1})

$v_1v_2v_3$		$v_1v_2v_3$		$v_1v_2v_3$	
(0,1,0)	812.50	(3,1,0)	3828.47	(0,1,2)	5154.77
(1,0,0)	1022.81	(0,5,0)	3930.93	(2,4,0)	5188.02
(0,2,0)	1612.17	(4,0,0)	4000.87	(3,0,1)	5255.18
(1,1,0)	1833.28	(1,1,1)	4034.91	(0,4,1)	5270.33
(2,0,0)	2028.77	(1,4,0)	4187.09	(0,7,0)	5408.96
(0,0,1)	2226.07	(2,0,1)	4260.11	(3,3,0)	5409.94
(0,3,0)	2398.69	(0,0,2)	4397.31	(1,0,2)	5440.33
(1,2,0)	2630.98	(3,2,0)	4416.87	(1,3,1)	5558.55
(2,1,0)	2837.44	(0,3,1)	4530.47	(4,2,0)	5611.93
(0,1,1)	3008.01	(3,2,0)	4624.21	(1,6,0)	5691.34
(3,0,0)	3021.10	(0,6,0)	4675.85	(5,1,0)	5795.58
(0,4,0)	3171.72	(1,2,1)	4800.02	(2,2,1)	5817.81
(1,0,1)	3253.60	(4,1,0)	4812.14	(0,2,2)	5905.17
(1,3,0)	3415.65	(1,5,0)	4945.19	(2,5,0)	5947.72
(2,2,0)	3633.47	(5,0,0)	4973.85	(6,0,0)	5974.25
(0,2,1)	3776.41	(2,1,1)	5041.20	(0,5,1)	5996.55

values of the L_z and L_z^2 operators were set to unity. In the Hamiltonian, the value of the spin orbit parameter A_{SO} has been kept constant (273 cm^{-1}) as calculated at the CASSCF level for the $^2\Pi$ equilibrium geometry (cf. Table 1). In these computations the s,p,d subset of the cc-pVQZ basis for the heavy atoms and s,p subset for hydrogen was used. The same ansatz yielded for the $X^2\Pi$ state of the NS radical a spin–orbit constant of 213 cm^{-1} as compared to the experimental value of 221.5 cm^{-1} [27] and for the excited $^3\Pi$ state of NS^+ a calculated value of 288 cm^{-1}. The increase of the splitting between the spin components in the linear HNS^+ relative to NS is clearly due to the fact that the triatom correlates with the $H + NS^+$ ($^3\Pi$) asymptote.

The calculations have been performed for $J = 1/2$, 3/2, 5/2 and 7/2, i.e. for K_a from 0 to 3. In Tables 6 and 7, the rovibronic levels ($N = K_a$) for the X state and ($N = K$) for the A state up to 6000 cm^{-1} are given. The assignments with harmonic quantum numbers were made according to the weight of the dominating vibrational configuration in the wave function. In linear/bent systems, the Renner–Teller coupling manifests itself in the K-reordering. In the bending levels of the X-state, K_a reordering begins in the $v_2 = 3$ level, for which the $K_a = 1$ state for the first time lies lower than the $K_a = 0$ state with the same bending quantum number. Already in the $v_2 = 2$ level, however, states with $K_a = 1$ and $K_a = 0$ come close together. Another consequence of this coupling is the 'saw-tooth' variation of the spin–orbit splitting. For the pure bending levels in both electronic components, this behaviour is shown in Fig. 5 where the splitting between the two F_1 and F_2 components are given as a function of the bending quantum number, v_2. Due to the remaining computational errors particularly in the barrier height and also in the shape of the PEF's the rovibronic levels given in Tables 6 and 7 represent the first information about their structure and the onset of a strong Renner–Teller coupling, but they have not yet the precision needed for exact attributions of spectral data.

In Table 8, the vibrational levels ($J = 0$) for HSN^+ calculated from a similar MRCI PEF expansion as for the other isomer are given. Also in this case, the nuclear motion problem has been solved variationally [33]. One can notice that the S–H stretch has been calculated to lie about 1000 cm^{-1} lower than the N–H stretch in the other isomer, the bending about 100 cm^{-1} higher and the N–S stretch 220 cm^{-1} lower. Both isomers are clearly distinguishable not only by their rotational stacks, but also by the different transition energies of their fundamental vibrations.

5. The protonation of the NS radical

In Figs. 2 and 3, colinear cuts of the CASSCF PEF's for the formation of both isomers are shown, for doublet and quartet states. Due to many close lying states of the NS^+ ion at this level of theory, we have calculated five asymptotes involving NS^+ below the $H^+ + NS$ asymptote. Though the energetic position of the close lying states in the triatomic species is probably not fully correct, the protonation of NS in its electronic ground state starting on the $^2\Pi$ PEF will cross quartet states and several conical intersection regions before reaching the bent HNS^+ minimum or the lowest $H(^2S) + NS^+(X^1\Sigma^+)$ asymptote. Equally complex will be the charge transfer processes between H and NS^+. Figs. 2 and 3 give an information about the characteristics of the electronic states, particularly one can distinguish between repulsive and bound electronic states. In the highly excited states, avoided crossings with the states of the same symmetry lead to additional complications.

6. Conclusions

Accurate values for proton affinity of NS and dissociation energies of the electronic ground state of HNS^+ and HSN^+ yielding $NS^+ + H$ are reported. The RCCSD(T) equilibrium structures of both isomers could serve to identify both isomers by microwave spectroscopy. The structure of the rovibronic levels in the Renner–Teller pair of the HNS^+ and vibrational anharmonic levels of HSN^+ are discussed. The present theoretical contribution could aid future spectroscopic experiments on both isomers.

Acknowledgements

This work has been supported by a scientific cooperation program: PICS (Programme International de Coopération Scientifique) between: Laboratoire de Physique des Lasers, Atomes et Molécules, Université de Lille 1, France, Laboratoire de Chimie Théorique, Université de Marne la Vallée, France, Damap, Observatoire de Paris-Meudon, France and Laboratoire de Physique Atomique et Moléculaire, Faculté des Sciences de Tunis, Tunisie.

References

[1] M. Houde, R. Peng, T.G. Phillips, P. Bastien, H. Yoshida, Astrophys. J. 537 (2000) 245.
[2] C. Sanchez Contreras, V. Bujarrabal, R. Neri, J. Alcolea, Astron. Astrophys. 357 (2000) 651.
[3] D. McGonagle, W.M. Irvine, Astrophys. J. 477 (1997) 711.
[4] T.J. Millar, in: T. Hartquist (Ed.), Molecular Astrophysics, Cambridge University Press, Cambridge, 1990.
[5] W.W. Duley, T.J. Miller, D.A. Williams, MNRAS 192 (1980) 945.
[6] C.A. Gottlib, J.A. Ball, E.W. Gottlib, C.J. Lada, H. Penfield, Astrophys. J. 200 (1975) L147.
[7] D. McGonagle, W.M. Irvine, M. Ohishi, Astrophys. J. 422 (1994) 621.
[8] W.M. Irvine, A.J. Lovell, M. Senay, H.E. Matthews, R.B. Metz, R. Meler, D. Mc Gonagle, American Astronomical Society, DPS meeting, 1999.
[9] M.P.S. Collins, B.J. Duke, J. Chem. Soc. Dalton Trans. (1978) 277.
[10] A. Melhorn, J. Sauer, J. Fabian, R. Mayer, Phosphorus Sulfur 11 (1981) 325.
[11] J. Wasilewski, V. Staemmler, Inorg. Chem. 25 (1986) 4221.
[12] M.W. Schmidt, P.N. Truong, M.S. Gordon, J. Am. Chem. Soc 109 (1987) 5217.
[13] R. Vetter, A. Mehlhorn, J. Mol. Struct. (THEOCHEM) 206 (1990) 11.
[14] P. Redondo, J.R. Flores, J. Largo-Cabrerizo, J. Comp. Chem. 10 (1989) 295.
[15] J.D. Watts, M.J. Huang, J. Phys. Chem. 99 (1995) 5331.
[16] A. Mehlhorn, J. Fabian, W. Gabriel, P. Rosmus, J. Mol. Struct. 339 (1995) 219.
[17] M.T. Nguyen, L.G. Vanquickenborne, M. Plisnier, R. Flammang, Mol. Phys. 78 (1993) 111.
[18] P.J. Bruna, G. Hirsch, Mol. ions, geometric, electronic structures, NATO ASI Ser., Ser. B: Phys. 90 (1983) 309.
[19] P. Gersdorf, J. Phys. Chem. A 101 (1997) 8778.
[20] J.M. Dyke, A. Morris, I.R. Trickle, J. Chem. Soc. Faraday Trans. II 73 (1977) 147.
[21] T.H. Dunning, J. Chem. Phys. 90 (1989) 1007.
[22] H.J. Werner, P.J. Knowles, J. Chem. Phys. 82 (1985) 5053.
[23] P.J. Knowles, H.J. Werner, Chem. Phys. Lett. 115 (1985) 259.
[24] H.J. Werner, P.J. Knowles, J. Chem. Phys. 89 (1988) 5803.
[25] P.J. Knowles, H.J. Werner, J. Chem. Phys. 145 (1988) 514.
[26] P.J. Knowles, C. Hampel, H.J. Werner, J. Chem. Phys. 99 (1993) 5219.
[27] K.P. Huber, G. Herzberg, Molecular Spectra and Molecular Structure: IV Constants of Diatomic Molecules, Van Nostrand Reinhold, New York, 1979.
[28] S.P. Karna, F. Grein, Chem.Phys. 109 (1986) 35.
[29] A. Karpfen, P. Schuster, J. Petkov, H. Lischka, J. Chem. Phys. 68 (1978) 3884.
[30] A.R. Hoy, I.M. Mills, G. Strey, Mol. Phys. 24 (1972) 1265.
[31] H.H. Nielsen, in: H. Flügge (Ed.), Handbuch der Physik, vol. 37, Springer, Berlin, 1959.
[32] S. Carter, N.C. Handy, P. Rosmus, G. Chambaud, Mol. Phys. 71 (1990) 605.
[33] S. Carter, N.C. Handy, Mol. Phys. 52 (1984) 1367.